

# Single Channel Characterization of the Mitochondrial Ryanodine Receptor in Heart Mitoplasts<sup>\*§</sup>

Received for publication, March 31, 2011, and in revised form, April 19, 2011. Published, JBC Papers in Press, April 27, 2011, DOI 10.1074/jbc.C111.245597

Shin-Young Ryu<sup>‡§</sup>, Gisela Beutner<sup>‡</sup>, Kathleen W. Kinnally<sup>§</sup>, Robert T. Dirksen<sup>‡</sup>, and Shey-Shing Sheu<sup>\*¶1</sup>

From the <sup>‡</sup>Department of Pharmacology and Physiology, University of Rochester Medical Center, Rochester, New York 14642, the

<sup>§</sup>Department of Basic Sciences, New York University, New York, New York 10010, and the <sup>¶</sup>Center for Translational Medicine, Department of Medicine, Thomas Jefferson University, Philadelphia, Pennsylvania 19107

Heart mitochondria utilize multiple  $\text{Ca}^{2+}$  transport mechanisms. Among them, the mitochondrial ryanodine receptor provides a fast  $\text{Ca}^{2+}$  uptake pathway across the inner membrane to control “excitation and metabolism coupling.” In the present study, we identified a novel ryanodine-sensitive channel in the native inner membrane of heart mitochondria and characterized its pharmacological and biophysical properties by directly patch clamping mitoplasts. Four distinct channel conductances of ~100, ~225, ~700, and ~1,000 picosiemens (pS) in symmetrical 150 mM CsCl were observed. The 225 pS cation-selective channel exhibited multiple subconductance states and was blocked by high concentrations of ryanodine and ruthenium red, known inhibitors of ryanodine receptors. Ryanodine exhibited a concentration-dependent modulation of this channel, with low concentrations stabilizing a subconductance state and high concentrations abolishing activity. The 100, 700, and 1,000 pS conductances exhibited different channel characteristics and were not inhibited by ryanodine. Taken together, these findings identified a novel 225 pS channel as the native mitochondrial ryanodine receptor channel activity in heart mitoplasts with biophysical and pharmacological properties that distinguish it from previously identified mitochondrial ion channels.

Mitochondrial  $\text{Ca}^{2+}$  transport plays critical roles in the regulation of mitochondrial function under both physiological and pathological conditions (1–3). An increase of matrix  $\text{Ca}^{2+}$  within the physiological range facilitates ATP production (4) by stimulating the activity of  $\text{Ca}^{2+}$ -dependent dehydrogenases (5, 6) in the tricarboxylic acid cycle and the ATP synthase (7). Dysregulation of mitochondrial  $\text{Ca}^{2+}$  handling and subsequent alterations in bioenergetics contribute to contractile dysfunction in heart failure (8, 9). Moreover, mitochondrial  $\text{Ca}^{2+}$  overload during ischemia/reperfusion induces opening of the mitochondrial permeability transition pore (mPTP),<sup>2</sup> mitochondrial

swelling, and an increase of reactive oxygen species generation, all of which lead to cardiac cell death (10, 11).

Several  $\text{Ca}^{2+}$  transport pathways have been identified. The mitochondrial  $\text{Ca}^{2+}$  uniporter (MCU) is a large capacity, low affinity system that provides a slow  $\text{Ca}^{2+}$  uptake mechanism (12). A highly  $\text{Ca}^{2+}$  selective, inwardly rectifying conductance with biophysical properties similar to those expected of the MCU was characterized in elegant patch clamp studies of mitoplasts isolated from Cos-7 cells (13) and human cardiomyocytes (14). Recently, *MICU1*, a gene encoding an EF hand protein that regulates MCU, was identified (15). However, heart mitochondria are also known to exhibit rapid  $\text{Ca}^{2+}$  uptake and efflux pathways that possess  $\text{Ca}^{2+}$  sensitivity and pharmacology different from those of the MCU (3).

We previously reported that a ryanodine-sensitive, fast  $\text{Ca}^{2+}$  uptake pathway co-exists with MCU in heart mitochondria (16, 17). High affinity binding of [<sup>3</sup>H]ryanodine, immunogold staining, and Western blot analysis revealed that a low level of functional ryanodine receptors is localized within the inner membrane of heart mitochondria (16). Interestingly, mitochondrial ryanodine receptor (mRyR) has characteristics different from those of ryanodine receptors located in the cardiac sarcoplasmic reticulum (SR) (16–18). The immunoreactivity of mRyR to type 1 RyR (RyR1) specific antibodies and the absence of mRyR in hearts from RyR1 knock-out mice are consistent with the molecular identity of mRyR as RyR1, and not the cardiac SR type 2 RyR isoform (RyR2) (17).

Ryanodine-sensitive channel activity was observed following incorporation in lipid bilayers of mRyRs purified from the inner membrane fraction of heart mitochondria (18). RyR1, but not RyR2, activity was recorded. Neither SR nor mitochondrial outer membrane markers were detected in these mRyR preparations. Nevertheless, potential low level contamination in these reconstitution experiments cannot be entirely excluded.

Patch clamping of mitoplasts allows characterization of the native ion channel activities and provides a direct means of conclusively determining whether the mRyR is located in the inner membrane (19). Although this technique is challenging due to the size and channel complexity of mitoplasts, several ion channels have been successfully identified using this approach (13, 14, 20, 21). However, the native biophysical prop-

\* This work was supported, in whole or in part, by National Institutes of Health Grants HL-033333 and HL-093671 (to S.-S. S.), AR-44657 (to R. T. D.), and GM57249 (to K. W. K.) and American Heart Association Postdoctoral Fellowship Grant 0525951T to S.-Y. R.

§ The on-line version of this article (available at <http://www.jbc.org>) contains supplemental Figs. 1–3.

<sup>1</sup> To whom correspondence should be addressed: 1025 Walnut St., Philadelphia, PA 19107. Tel.: 215-503-5152; Fax: 215-503-5731; E-mail: shey-shing.sheu@jefferson.edu.

<sup>2</sup> The abbreviations used are: mPTP, mitochondrial permeability transition pore; RyR, ryanodine receptor; mRyR, mitochondrial ryanodine receptor; MCU, mitochondrial  $\text{Ca}^{2+}$  uniporter; SR, sarcoplasmic reticulum; mCS,

mitochondrial centum picosiemens channel; TIM, translocase of inner membrane; CsA, cyclosporin A; BKA, bongkreic acid; FKBP, FK-506-binding protein; pS, picosiemens(s); RuR, ruthenium red; COX, cytochrome c oxidase.

erties of mRyR in mitoplasts have not previously been reported. In the present study, we characterized the biophysical and pharmacological properties of native single mRyR channels in heart mitoplasts that are distinct from those of several other large conductance channels.

## EXPERIMENTAL PROCEDURES

**Isolation of Heart Mitochondria and Preparation of Mitoplasts**—Mitochondria were obtained from cardiomyocytes isolated from whole hearts of 2–3-month-old Sprague-Dawley rats following homogenization and differential centrifugation in a mannitol-sucrose buffer (in mM: 70 sucrose, 225 mannitol, 10 HEPES, 1 EGTA, pH 7.2, with KOH, and 1 mg/ml fatty acid-free bovine serum albumin) as described previously (16, 17). Isolated mitochondria were transferred to a hypotonic solution (in mM: 5 sucrose, 5 HEPES, 1 EGTA, pH 7.2, with KOH) and kept on ice for 5 min to form mitoplasts. Mitoplasts were sedimented at 10,000 rpm with a tabletop centrifuge (Eppendorf) for 5 min and transferred to an isotonic KCl solution (in mM: 150 KCl, 10 HEPES, 1 EGTA, pH 7.2, with KOH). All the procedures were performed on ice. All animals were carefully handled, anesthetized, and sacrificed in accordance with guidelines of the National Institutes of Health, and protocols were approved by the University Committee on Animal Resources at the University of Rochester Medical Center.

**Fluorescence Microscopy**—Cardiomyocytes were isolated by collagenase (type II, Worthington) treatment using a Langendorff perfusion system, as described previously (22). Single intact cardiomyocytes were stained with 100 nM MitoTracker Red CM-H<sub>2</sub>XRos (Invitrogen) for 30 min. After washing cardiomyocytes twice with a modified normal Tyrode's solution (in mM: 143 NaCl, 5.4 KCl, 1.8 CaCl<sub>2</sub>, 0.5 MgCl<sub>2</sub>, 10 glucose, 5 HEPES, pH 7.4, with NaOH), mitochondria and mitoplasts were prepared as described above. Fluorescence images of MitoTracker Red staining were captured following excitation at 550 nm with a monochromator (Polychrome IV, TILL Photonics) and a >600 nm emission using a digital CCD camera (TILL Imago CCD camera, TILL Photonics) and Plan Apo ×60 oil emersion objective (numerical aperture 1.4, Nikon) attached to an inverted microscope (TE2000-S, Nikon).

**Patch Clamping of Mitoplasts**—1–2 μl of mitoplast-containing solution was placed undisturbed for several minutes on a glass bottom chamber to allow mitoplasts to settle to the bottom of the chamber. Bath recording solution (in mM: 150 CsCl, 5 HEPES, pH 7.2, with CsOH) was then carefully added to minimally disrupt attached mitoplasts. Mitoplasts appeared as transparent vesicles with a diameter of 2–5 μm and a “cap” region, reflecting remnants of the outer membrane, when viewed using a phase contrast microscope (Nikon Diaphot inverted, Nikon Instruments Inc.). The transparent membrane portion of the mitoplast, away from the cap region, was approached using patch clamp micropipettes fabricated from borosilicate glass capillaries (1B100F-4, World Precision Instruments) generated using a horizontal puller (P-87, Sutter Instrument Co.). The patch clamp pipettes exhibited resistances of 15–20 megaohms when filled with the pipette recording solution (in mM: 150 CsCl, 5 HEPES, pH 7.2, with various free Ca<sup>2+</sup> concentrations adjusted with CaCl<sub>2</sub> and EGTA). Data

were collected using the pClamp 9.2 software, a patch clamp amplifier (Axopatch 200B, Axon Instruments), and a 16-bit digitizer (Digidata 1322A, Axon Instruments). Signals were filtered at 1–5 kHz with a built-in low pass filter and digitized at 2–10 kHz. Data were analyzed offline using Clampfit 9.2 (Axon Instruments) and Origin 8.0 (OriginLab Corp.). All recordings were made from inside-out excised patches with membrane voltages reported as matrix voltage. All experiments were conducted at 25 ± 1 °C to enable comparison with the biophysical properties of various previously reported mitochondrial ion channels.

**Drugs and Peptides**—Cyclosporin A (CsA), ruthenium red (RuR), and 4,4'-diisothiocyanostilbene-2,2'-disulfonate were purchased from Sigma. Ru360 was purchased from Calbiochem. Ryanodine and bongkreikic acid (BKA) were purchased from Enzo Life Sciences. Mitochondrial targeting presequence peptides used were based on amino acids 1–13 and 1–22 from the N terminus of cytochrome oxidase subunit IV of *Saccharomyces cerevisiae* (γCOX-IV<sub>1–13</sub> and γCOX-IV<sub>1–22</sub>). Peptides were prepared by the New York State Department of Health Wadsworth Center Peptide Synthesis Core Facility (Albany, NY) using an Applied Biosystems 431A automated peptide synthesizer as described previously (23).

**Statistical Analysis**—Statistical significance was determined using a two-tailed Student's *t* test with an assumption of equal variance using Origin 8.0 software (OriginLab) with *p* < 0.05 considered statistically significant. Data are presented as mean ± S.D. unless mentioned otherwise. *n* indicates the number of experiments.

## RESULTS

**Ryanodine-sensitive Channel Activity in Heart Mitoplasts**—To confirm that our mitoplast preparations were indeed derived from cardiac mitochondria, we stained freshly isolated cardiomyocytes with MitoTracker Red CM-H<sub>2</sub>XRos and then examined mitoplasts isolated from these myocytes under a fluorescence microscope. The membrane potential-dependent accumulation of MitoTracker Red allowed visualization of mitochondria within intact cardiomyocytes (Fig. 1A, panel a). The fluorescence of this fixable mitochondrial probe, MitoTracker Red, remained associated with mitochondria and mitoplasts throughout isolation (Fig. 1A). Under bright field microscopy, isolated mitochondria appeared as small and optically dense spheres (Fig. 1A, panel b), often less than 1 μm in diameter. Mitoplasts were formed by hypotonic treatment, during which time mitochondrial swelling resulted in exposure of the mitochondrial inner membrane. Mitoplasts appeared as transparent vesicles 2–5 μm in diameter that typically had a black spot, or cap, reflecting remnants of the outer membrane, on one side (Fig. 1A, panel c).

Most recordings of ryanodine-sensitive channel activity in heart mitoplasts were obtained using Cs<sup>+</sup>-containing solutions to exclude several K<sup>+</sup>-selective channels (24–26) including mitochondrial ATP-sensitive (mitoK<sub>ATP</sub>) (27–29) and Ca<sup>2+</sup>-activated (mitoK<sub>Ca</sub>) K<sup>+</sup> channels (21). In symmetrical 150 mM CsCl, four large conductance channel activities were observed with different detection frequencies in heart mitoplasts (Fig.

## Mitochondrial Ryanodine Receptor

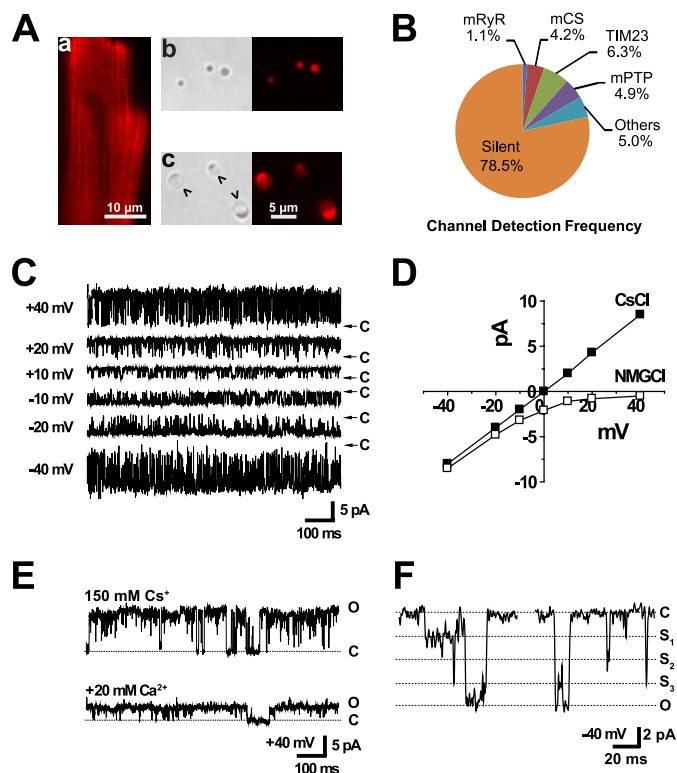


**FIGURE 1. Properties of ryanodine-sensitive channel activity recorded from heart mitoplasts.** Mitoplasts were generated from mitochondria isolated from rat heart, and the exposed inner membrane was patch clamped. *A*, images are shown during the preparation of heart mitoplasts. *Panel a*, a fluorescence image is shown for an intact cardiomyocyte in which mitochondria were visualized by staining with 100 nM MitoTracker Red CM-H<sub>2</sub>XRos. *Panels b* and *c*, representative phase contrast and fluorescence images of mitochondria (*panel b*) and mitoplasts (*panel c*) are shown. *Arrowheads* indicate regions of exposed inner membrane in a mitoplast that was patched with a micropipette. The scale bar is 10  $\mu\text{m}$  in *panel a* and 5  $\mu\text{m}$  in *panels b* and *c*. *B*, channel detection frequencies out of total 1,152 independent patches in heart mitoplasts with symmetrical 150 mM CsCl. When a mitochondrial targeting sequence peptide, yCOX-IV, was included in the pipette recording solution, the TIM23 channel activity was observed in 9 out of 45 patches (20% detection frequency, not shown). *C*, representative single channel current traces of 225 pS channel activity from an excised inside-out patch recorded at the indicated voltages (from  $-40$  to  $+40$  mV) using symmetrical 150 mM CsCl solutions and 100  $\mu\text{M}$  free  $\text{Ca}^{2+}$  in the patch pipette. *D*, current-voltage plot is shown for a representative mRyR channel in symmetrical 150 mM CsCl and after replacement of  $\text{Cs}^+$  in the bath solution with equimolar *N*-methyl-D-glucamine (NMG). *E*, representative single channel current traces are shown before and after the addition of 20 mM  $\text{Ca}^{2+}$  to the bath solution. *F*, representative single channel current trace of the 225 pS conductance channel showing multiple subconductance states. *O*, *S*<sub>1</sub>–*S*<sub>3</sub>, and *C* indicate fully open, subconductance, and closed states, respectively.

1*B*). These activities include channels with maximum conductances of 100, 225, 700, and 1,000 pS.

The 225 pS conductance channels were cation-selective, calcium-sensitive, and inhibited by high concentrations (100  $\mu\text{M}$ ) of ryanodine (Figs. 1 and 2) ( $n = 13$ ). The maximum single channel conductance showed a linear current-voltage relationship in symmetrical 150 mM CsCl with 100  $\mu\text{M}$  free  $\text{Ca}^{2+}$  in the patch pipette internal solution (Fig. 1*C*). The 225 pS channel is cation-selective because outward conductance through the channel is abolished by substituting  $\text{Cs}^+$  in the bath (*i.e.* matrix side) recording solution with *N*-methyl-D-glucamine (Fig. 1*D*). This channel is apparently permeable to  $\text{Ca}^{2+}$  as the addition of 20 mM  $\text{CaCl}_2$  to the bath solution markedly decreased the cesium-based single channel conductance from 225 to 50 pS (Fig.

1*E*). The 225 pS channel also showed multiple conductance states including a closed, a fully open, and at least three subconductance states (Fig. 1*F*). Individual single channel current traces often showed direct transitions from the fully open/closed state to one of the different subconductance levels.

**Pharmacological Properties of the 225 pS Channel**—One of the unique features of ryanodine receptors is their specific and concentration-dependent sensitivity to ryanodine (30). Low concentrations (1–10  $\mu\text{M}$ ) of ryanodine lock the channel into a long-lived subconductance open state (31), whereas high concentrations ( $\geq 100$   $\mu\text{M}$ ) block the channel from opening (32). We determined whether the 225 pS channel activity was similarly modulated by different concentrations of ryanodine. To calculate open probability ( $P_o$ ) and mean open time, the threshold was set to include any subconductance or open state. In control conditions, with 20  $\mu\text{M}$   $\text{Ca}^{2+}$  in pipette, the  $P_o$  and mean open time were initially  $0.15 \pm 0.04$  and  $1.63 \pm 0.42$  ms, respectively ( $n = 3$ ). The addition of 10  $\mu\text{M}$  ryanodine stabilized a long-lasting subconductance opening of the 225 pS channel (Fig. 2, *A* and *B*). The  $P_o$  and mean open time were increased to  $0.83 \pm 0.04$  and  $5.7 \pm 1.7$  ms, respectively ( $n = 3$ ). The open dwell time histograms were well fitted by a two-exponential decay function (Fig. 2*C*). The fast and slow time constants from the fit of the open dwell time histogram were increased from  $\tau_1 = 0.7 \pm 0.1$  ms and  $\tau_2 = 3.0 \pm 0.9$  ms to  $\tau_1 = 1.1 \pm 0.3$  ms and  $\tau_2 = 8.3 \pm 3.3$  ms by 10  $\mu\text{M}$  ryanodine ( $n = 3$ ) (Fig. 2*C*). Further addition of 100  $\mu\text{M}$  ryanodine completely inhibited the channel activity ( $P_o \sim 0$ ) (Fig. 2, *A* and *B*). Based on these results, we will hereafter refer to the ryanodine-sensitive 225 pS channel as the mRyR. Preincubation with 10  $\mu\text{M}$  Ru360, an inhibitor of the MCU, did not block mRyR channel activity, but the addition of 5  $\mu\text{M}$  RuR, a nonspecific inhibitor of both ryanodine receptors and the MCU, abolished mRyR channel activity (Fig. 2*D*) ( $n = 3$ ).

The mPTP exhibits a large single channel conductance of  $\sim 1,000$  pS. However, because mPTP also has multiple subconductance open states (33, 34), we tested whether the 225 pS mRyR channel activity was blocked by inhibitors of the mPTP. We found that mPTP inhibitors CsA (5  $\mu\text{M}$ ) and BKA (20  $\mu\text{M}$ ) had no direct effect on the 225 pS conductance channel ( $n = 4$ ) (Fig. 2*E*), indicating that mRyR channel activity does not reflect a subconductance of the mPTP. Fig. 2*F* summarizes the pharmacological properties of mRyR. The results presented in Figs. 1 and 2 provide a biophysical and pharmacological fingerprint of the 225 pS channel and support its identification as mRyR.

**Comparison of mRyR Channel Activity with That of Other Channels Recorded in Heart Mitoplasts**—In addition to the 225 pS mRyR channel activity, we also routinely recorded channels with conductances of  $\sim 100$ ,  $\sim 700$ , and  $\sim 1,000$  pS in heart mitoplasts. We compared the biophysical and pharmacological properties of these channel activities with those of the mRyR.

The 100 pS conductance channel exhibited characteristics typical of the mitochondrial centum picosiemens conductance channel (mCS) (20, 35). This channel activity showed high  $P_o$  at positive voltages, whereas the channel remained predominantly closed with a low  $P_o$  at negative voltages (supplemental Fig. 1, *A* and *B*). The mCS channel activity was not sensitive to

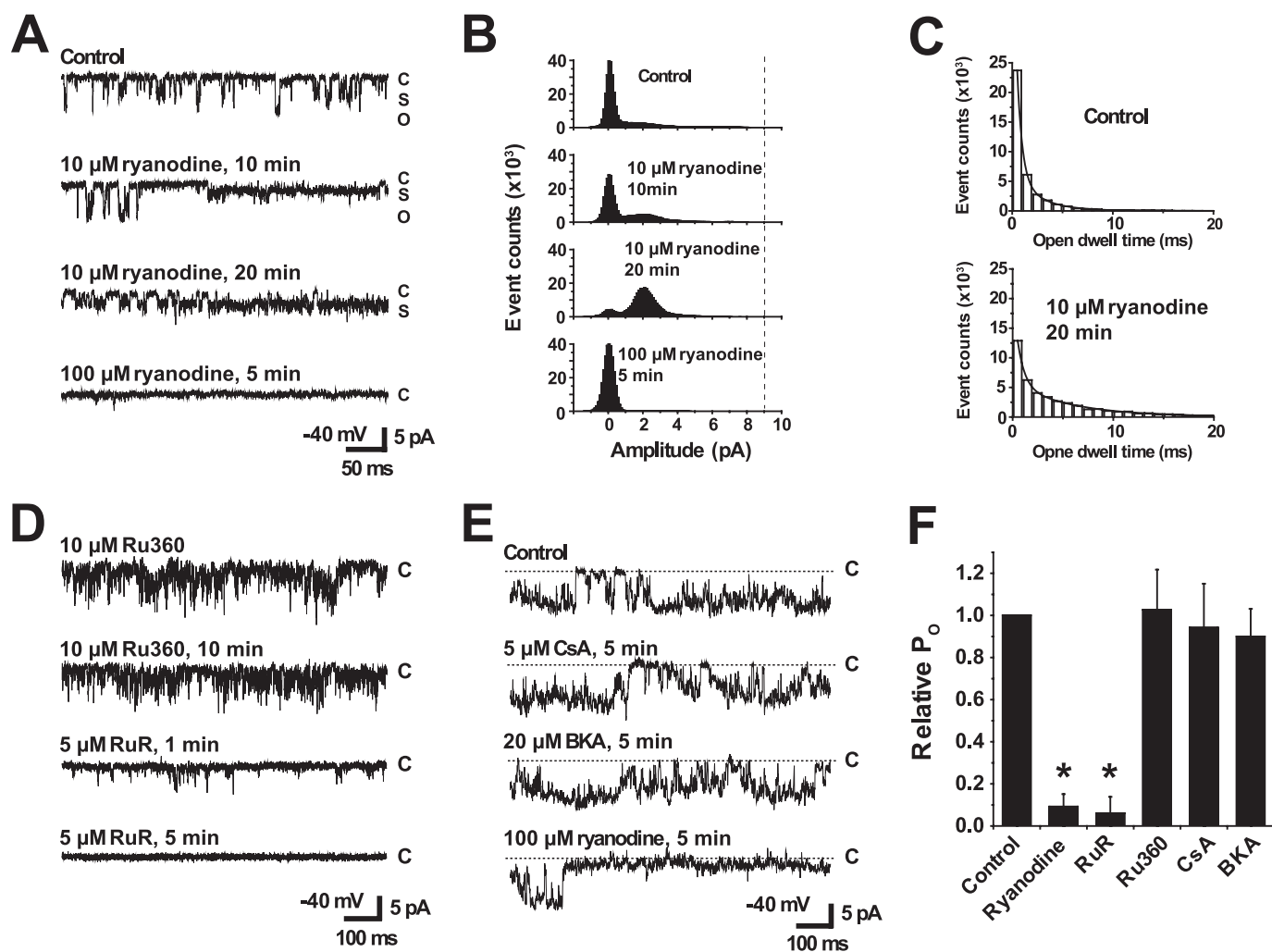


**FIGURE 2. Pharmacological properties of mRyR channel activity.** Heart mitoplasts were patch clamped in symmetrical 150 mM CsCl. Current traces recorded at  $-40$  mV (openings reflected by downward deflections) show the effects of various pharmacological agents. *A*, representative current traces are shown before (*top trace*), 10 and 20 min after the addition of  $10 \mu\text{M}$  ryanodine (*middle two traces*), and finally after the addition of  $100 \mu\text{M}$  ryanodine (*bottom trace*). The pipette solution contained  $20 \mu\text{M}$   $\text{Ca}^{2+}$ . *C*, *O*, and *S* indicate closed, open, and subconductance states, respectively. All other recording conditions are identical as in Fig. 1. *B*, all points amplitude histograms of 30 s of corresponding current traces in the experiment shown in *A* for control, 10 and 20 min after the addition of  $10 \mu\text{M}$  ryanodine, and finally after the addition of  $100 \mu\text{M}$  ryanodine. Increased frequency of subconductance openings are observed for mRyR during the application of  $10 \mu\text{M}$  ryanodine. The vertical dotted line indicates maximum single channel current amplitude. *C*, open dwell time histograms before (*Control, upper*) and 20 min after the addition of  $10 \mu\text{M}$  ryanodine (*lower*). Histograms were fitted with a two-exponential decay function,  $y = A_1 \times \exp(-x/\tau_1) + A_2 \times \exp(-x/\tau_2) + C$ , to obtain fast ( $\tau_1$ ) and slow ( $\tau_2$ ) time constants.  $x$  is the dwell time (in ms). *D*, single channel activity of mRyR after the addition of  $10 \mu\text{M}$  Ru360 followed by the addition of  $5 \mu\text{M}$  RuR. Pipette solution contained  $50 \mu\text{M}$   $\text{Ca}^{2+}$ . *E*, effects on mRyR channel activity of sequential bath perfusion of  $5 \mu\text{M}$  CsA and then  $20 \mu\text{M}$  BKA.  $100 \mu\text{M}$  ryanodine was added at the end of the experiment to confirm channel identity as mRyR. Pipette solution contained  $100 \mu\text{M}$   $\text{Ca}^{2+}$ . *F*, average ( $\pm$  S.E.) relative mRyR channel open probability after various drug treatments ( $n = 3$ –13 patches). The asterisks indicate  $p < 0.05$ .

$100 \mu\text{M}$  ryanodine but was completely inhibited by  $50 \mu\text{M}$  4,4'-diisothiocyanostilbene-2,2'-disulfonate, a broad spectrum anion channel inhibitor (supplemental Fig. 1C,  $n = 3$ ).

The protein import complex, translocase of inner membrane, TIM23 contains a targeting peptide-sensitive and voltage-dependent channel. The TIM23 channel has a maximum conductance of 700–800 pS and a half-open state of 350–400 pS (23, 36, 37). We recorded a  $\sim 700$  pS channel that was primarily present in either the half-open or the fully closed state at positive voltages ( $+40$  and  $+80$  mV) but mostly in the fully open state at negative voltages (supplemental Fig. 2, *A* and *B*). Although the addition of  $100 \mu\text{M}$  ryanodine had no effect on this channel activity (supplemental Fig. 2C,  $n = 5$ ), the 700 pS conductance channel was observed more frequently, 9 out of 45 patches (20% detection

frequency), in patches when a mitochondrial targeting sequence peptide,  $\gamma\text{COX-IV}$ , was included in the pipette recording solution. These findings indicate that the 700 pS conductance channel corresponds to the protein import channel of inner membrane, TIM23 (38, 39).

The  $\sim 1,000$  pS conductance channel showed characteristics consistent with mPTP activity (33, 40), which exhibits a very large single channel conductance with multiple subconductance states (supplemental Fig. 3). This channel activity was inhibited by CsA but was unaltered by  $100 \mu\text{M}$  ryanodine (supplemental Fig. 3,  $n = 3$ ). Taken together, these results indicate that mRyR channel activity exhibits unique biophysical and pharmacological properties that distinguish it from other large conductance ion channel activities previously reported in heart mitoplasts.

### DISCUSSION

In the present study, we identified a novel  $\text{Ca}^{2+}$ -permeable and ryanodine-sensitive mitochondrial channel (referred to as mRyR) in heart mitoplasts. The mRyR is a voltage-independent and cation-selective channel with a maximum single channel conductance of 225 pS in symmetrical 150 mM CsCl. The mRyR channel activity is differentially modulated by ryanodine, with low concentrations stabilizing a low subconductance state and high concentrations stabilizing the fully closed state. The absence of sensitivity to BKA or CsA indicates that this mRyR channel activity does not reflect subconductance openings of mPTP. Other channel activities observed in heart mitoplasts under our recording conditions, including mCS, TIM23, and mPTP, were not sensitive to ryanodine and exhibited biophysical properties distinct from that of mRyR. This study provides the first characterization of the biophysical and pharmacological properties of native mRyR channels directly recorded from freshly prepared heart mitoplasts.

The single channel conductance of mRyR channel activity is slightly smaller than that reported for SR RyR channels incorporated into planar lipid bilayers. Ryanodine receptors purified from the SR membrane of skeletal and cardiac muscle exhibit large single channel conductances of 400–750 pS in 250 mM  $\text{K}^+$  or  $\text{Cs}^+$  (30, 41). Previously, we reported that ryanodine-sensitive activities purified from rat heart mitochondria and reconstituted into lipid bilayers exhibited single channel conductances of  $\sim$ 500–800 pS with symmetrical 300 mM cesium methanesulfonate (18). Considering the reduced ionic strength in the present patch clamp experiments, we expected conductances of  $\sim$ 250–400 pS but saw 225 pS of activity in symmetrical 150 mM CsCl conditions. We speculate that the smaller conductance observed here may in part be due to differential regulation by associated proteins present in mitoplasts when compared with the SR or lost during reconstitution into bilayers. The function of SR RyRs is modulated by interaction with a large number of associated proteins including calmodulin, triadin, junctin, calsequestrin, and FK-506-binding protein (FKBP) (30). Specifically, FKBP12 binds to the skeletal muscle SR ryanodine receptor (RyR1) (42), which is the same RyR subtype as mRyR in heart mitochondria (17), and binding of FKBP12 to RyR1 coordinates cooperative gating of the four RyR1 subunits, eliminating subconductance states and preferentially stabilizing the fully open and closed states of the channel. Although a small amount of FKBP12 is also expressed in cardiomyocytes, the FKBP12.6 isoform is thought to normally be bound to RyR2 in the cardiac SR (43). The level of FKBP12, FKBP12.6, or other related FKBP in cardiac mitochondria available to interact with mRyR is unknown. Thus, it will be important for future studies to identify the proteins that interact with mRyR and regulate mRyR gating and function.

Interestingly, our single channel studies identified at least four conductance levels for the mRyR, similar to those previously shown for the SR ryanodine receptor (44). We previously reported the molecular mass of mRyR under denaturing conditions to be  $\sim$ 500–600 kDa, a size similar to that of each subunit in the tetrameric structure of ryanodine receptor in the SR (16, 18). Thus, our results are consistent with mRyR being a homotetramer in which conformational changes in each subunit contribute equally to channel gating and conductance. The somewhat reduced unitary

conductance and subconductance gating of mRyR may serve to help maintain electrochemical gradients across the mitochondrial inner membrane during rapid  $\text{Ca}^{2+}$  uptake through the channel.

In the present study, mRyR channel activity was detected in  $\sim$ 1% of all successful inside-out patches obtained from heart mitoplasts (from 1,152 total patches), which is a low frequency when compared with that of the other large conductance channels observed in this study (Fig. 1B). Assuming the diameter of a circular mitoplast and that the openings of the patch pipette are 5 and 0.5  $\mu\text{m}$ , respectively, the surface area of a mitoplast is 400 times larger than the pore size of a patch pipette, 78.5 *versus* 0.196  $\mu\text{m}^2$ . From the detection frequency of mRyR and the ratio of surface area/pore size, the density of mRyR is calculated to be  $\sim$ 0.06/ $\mu\text{m}^2$ , or 4–5 channels in one mitochondrion. These calculations are consistent with our previous findings of both low frequency of mRyR detection by immunogold staining and low maximal density of [ $^3\text{H}$ ]ryanodine binding in purified mitochondria (16). This finding is physiologically important as a low mRyR channel density would be required to minimize depolarization of the mitochondrial membrane potential during rapid  $\text{Ca}^{2+}$  uptake used to enhance mitochondrial bioenergetics. However, we cannot exclude the possibility that the number and activity of functional mRyR channels may decrease as a result of mitoplast preparation and during inside-out patch clamp recording as is known to occur for other membrane ion channels (45–48). Defining the regulation of mRyR function by phosphorylation, redox status, and protein-protein interactions within the mitochondrial niche are important topics for future study. It should be noted that other investigators have previously reported the existence of a small amount of ryanodine receptors in mitochondria of liver (49), neurons (50), osteoblasts (51), and endothelial cells (52).

Our previous studies suggested that mRyR is maximally activated at 10–100  $\mu\text{M}$  cytosolic  $\text{Ca}^{2+}$  but inhibited at higher  $\text{Ca}^{2+}$  concentrations (3, 16). Unlike mRyR, MCU is not inhibited by high  $\text{Ca}^{2+}$  concentrations (3), exhibits high  $\text{Ca}^{2+}$  selectivity and a very small single channel conductance, and shows prominent inward rectification (13, 14). Thus, high  $\text{Ca}^{2+}$ -containing solutions (105 mM  $\text{Ca}^{2+}$ ) and very negative voltage pulses (*e.g.* –160 mV) have been used previously to record single channel activity of MCU (13, 14). MCU activity was not observed in our experiments because very low concentrations of free  $\text{Ca}^{2+}$  (20–100  $\mu\text{M}$ ) were used to record mRyR channel activity. We postulate that the unique  $\text{Ca}^{2+}$  dependence and relatively large single channel conductance of mRyR enable this channel to serve as a fast and transient mitochondrial  $\text{Ca}^{2+}$  uptake mechanism within the physiological range of  $\text{Ca}^{2+}$  elevations between SR and mitochondria in cardiomyocytes during beat-to-beat excitation-contraction coupling (3).

We propose that the primary role of mRyR is to mediate rapid mitochondrial  $\text{Ca}^{2+}$  uptake to regulate excitation and metabolism coupling in heart cells (3, 17, 18). However, mRyR may also serve as a  $\text{Ca}^{2+}$  efflux mechanism depending on the electrochemical gradient of  $\text{Ca}^{2+}$  across the inner membrane. In addition,  $\text{K}^+$  flux through mRyR may also act as an important regulator of mitochondrial energy metabolism. Aon *et al.* (53) suggested that a modest increase in  $\text{K}^+$  conductance through mitoK<sub>Ca</sub> channels, which exhibit a relatively large single chan-

nel conductance of  $\sim 300$  pS (21), enhances mitochondrial energetic performance. Accordingly,  $K^+$  influx through mRyR may enhance mitochondrial energy production by modulating matrix volume. The dynamic regulation of the mitochondrial membrane potential due to  $K^+$  flux may also limit mitochondrial  $Ca^{2+}$  overload during mRyR activation.

In summary, we identified a novel ryanodine-sensitive 225 pS channel, termed mRyR, in the native inner membrane of heart mitochondria. The present study significantly expands our understanding of mitochondrial ion transport mechanisms. Moreover, because dysregulation in mitochondrial  $Ca^{2+}$  handling is implicated in various cardiac disorders (8, 14, 54), it will be important for future studies to determine the potential role of altered mRyR function in cardiac development, heart failure, cardiomyopathy, and ischemia/reperfusion injury. Furthermore, if mRyR also operates in other tissues, including skeletal muscle and neurons,<sup>3</sup> altered mRyR function may also contribute to the pathophysiology of other human disorders including malignant hyperthermia, central core disease, and neurodegeneration.

*Acknowledgments*—We thank members of the Sheu and Dirksen laboratories and all members of Mitochondrial Research and Innovation Group in the University of Rochester Medical Center for critical comments. We also thank Dr. Yuriy Kirichok for critical comments.

## REFERENCES

- Brookes, P. S., Yoon, Y., Robotham, J. L., Anders, M. W., and Sheu, S. S. (2004) *Am. J. Physiol. Cell Physiol.* **287**, C817–C833
- Gunter, T. E., and Sheu, S. S. (2009) *Biochim. Biophys. Acta* **1787**, 1291–1308
- Ryu, S. Y., Beutner, G., Dirksen, R. T., Kinnally, K. W., and Sheu, S. S. (2010) *FEBS Lett.* **584**, 1948–1955
- Balaban, R. S. (2009) *Biochim. Biophys. Acta* **1787**, 1334–1341
- McCormack, J. G., and Denton, R. M. (1993) *Dev. Neurosci.* **15**, 165–173
- Denton, R. M. (2009) *Biochim. Biophys. Acta* **1787**, 1309–1316
- Das, A. M., and Harris, D. A. (1990) *Biochem. Soc. Trans.* **18**, 554–555
- Maack, C., and O'Rourke, B. (2007) *Basic Res. Cardiol.* **102**, 369–392
- Liu, T., and O'Rourke, B. (2008) *Circ. Res.* **103**, 279–288
- Di Lisa, F., and Bernardi, P. (2006) *Cardiovasc. Res.* **70**, 191–199
- Halestrap, A. P. (2009) *J. Mol. Cell Cardiol.* **46**, 821–831
- Gunter, T. E., Yule, D. I., Gunter, K. K., Eliseev, R. A., and Salter, J. D. (2004) *FEBS Lett.* **567**, 96–102
- Kirichok, Y., Krapivinsky, G., and Clapham, D. E. (2004) *Nature* **427**, 360–364
- Michels, G., Khan, I. F., Endres-Becker, J., Rottlaender, D., Herzig, S., Ruhparwar, A., Wahlers, T., and Hoppe, U. C. (2009) *Circulation* **119**, 2435–2443
- Perocchi, F., Gohil, V. M., Girgis, H. S., Bao, X. R., McCombs, J. E., Palmer, A. E., and Mootha, V. K. (2010) *Nature* **467**, 291–296
- Beutner, G., Sharma, V. K., Giovannucci, D. R., Yule, D. I., and Sheu, S. S. (2001) *J. Biol. Chem.* **276**, 21482–21488
- Beutner, G., Sharma, V. K., Lin, L., Ryu, S. Y., Dirksen, R. T., and Sheu, S. S. (2005) *Biochim. Biophys. Acta* **1717**, 1–10
- Altschaf, B. A., Beutner, G., Sharma, V. K., Sheu, S. S., and Valdivia, H. H. (2007) *Biochim. Biophys. Acta* **1768**, 1784–1795
- Grigoriev, S. M., Muro, C., Dejean, L. M., Campo, M. L., Martinez-Caballero, S., and Kinnally, K. W. (2004) *Int. Rev. Cytol.* **238**, 227–274
- Kinnally, K. W., Zorov, D. B., Antonenko, Y. N., Snyder, S. H., McEnery, M. W., and Tedeschi, H. (1993) *Proc. Natl. Acad. Sci. U.S.A.* **90**, 1374–1378
- Xu, W., Liu, Y., Wang, S., McDonald, T., Van Eyk, J. E., Sidor, A., and O'Rourke, B. (2002) *Science* **298**, 1029–1033
- Ryu, S. Y., Lee, S. H., and Ho, W. K. (2005) *J. Mol. Cell Cardiol.* **39**, 874–881
- Lohret, T. A., Jensen, R. E., and Kinnally, K. W. (1997) *J. Cell Biol.* **137**, 377–386
- Szewczyk, A., Jarmuszkiewicz, W., and Kunz, W. S. (2009) *IUBMB Life* **61**, 134–143
- O'Rourke, B. (2004) *Circ. Res.* **94**, 420–432
- Szewczyk, A., Skalska, J., Glab, M., Kulawiak, B., Malińska, D., Koszala-Piotrowska, I., and Kunz, W. S. (2006) *Biochim. Biophys. Acta* **1757**, 715–720
- Er, F., Michels, G., Gassanov, N., Rivero, F., and Hoppe, U. C. (2004) *Circulation* **110**, 3100–3107
- Garlid, K. D., Dos Santos, P., Xie, Z. J., Costa, A. D., and Paucek, P. (2003) *Biochim. Biophys. Acta* **1606**, 1–21
- Bednarczyk, P., Dołowy, K., and Szewczyk, A. (2005) *FEBS Lett.* **579**, 1625–1632
- Fill, M., and Copello, J. A. (2002) *Physiol. Rev.* **82**, 893–922
- Rousseau, E., Smith, J. S., and Meissner, G. (1987) *Am. J. Physiol.* **253**, C364–C368
- Zimányi, I., Buck, E., Abramson, J. J., Mack, M. M., and Pessah, I. N. (1992) *Mol. Pharmacol.* **42**, 1049–1057
- Szabó, I., and Zoratti, M. (1991) *J. Biol. Chem.* **266**, 3376–3379
- Zorov, D. B., Kinnally, K. W., Perini, S., and Tedeschi, H. (1992) *Biochim. Biophys. Acta* **1105**, 263–270
- Beavis, A. D., and Davatol-Hag, H. (1996) *J. Bioenerg. Biomembr.* **28**, 207–214
- Muro, C., Grigoriev, S. M., Pietkiewicz, D., Kinnally, K. W., and Campo, M. L. (2003) *Biophys. J.* **84**, 2981–2989
- Martinez-Caballero, S., Grigoriev, S. M., Herrmann, J. M., Campo, M. L., and Kinnally, K. W. (2007) *J. Biol. Chem.* **282**, 3584–3593
- Kushnareva, Y. E., Campo, M. L., Kinnally, K. W., and Sokolove, P. M. (1999) *Arch. Biochem. Biophys.* **366**, 107–115
- Murphy, R. C., Diwan, J. J., King, M., and Kinnally, K. W. (1998) *FEBS Lett.* **425**, 259–262
- Kinnally, K. W., Zorov, D., Antonenko, Y., and Perini, S. (1991) *Biochem. Biophys. Res. Commun.* **176**, 1183–1188
- Fill, M., Coronado, R., Mickelson, J. R., Vilven, J., Ma, J. J., Jacobson, B. A., and Louis, C. F. (1990) *Biophys. J.* **57**, 471–475
- Avila, G., Lee, E. H., Perez, C. F., Allen, P. D., and Dirksen, R. T. (2003) *J. Biol. Chem.* **278**, 22600–22608
- Timerman, A. P., Onoue, H., Xin, H. B., Barg, S., Copello, J., Wiederrecht, G., and Fleischer, S. (1996) *J. Biol. Chem.* **271**, 20385–20391
- Ahern, G. P., Junankar, P. R., and Dulhunty, A. F. (1997) *Biophys. J.* **72**, 146–162
- Xu, J. J., Hao, L. Y., Kameyama, A., and Kameyama, M. (2004) *Am. J. Physiol. Cell Physiol.* **287**, C1717–C1724
- Ono, K., and Fozzard, H. A. (1992) *J. Physiol.* **454**, 673–688
- Zhang, G., Xu, R., Heinemann, S. H., and Hoshi, T. (2006) *Biochem. Biophys. Res. Commun.* **342**, 1389–1395
- Rosenmund, C., and Westbrook, G. L. (1993) *J. Physiol.* **470**, 705–729
- Feng, L., Pereira, B., and Kraus-Friedmann, N. (1992) *Cell Calcium* **13**, 79–87
- Pickel, V. M., Clarke, C. L., and Meyers, M. B. (1997) *J. Comp. Neurol.* **386**, 625–634
- Sun, L., Adebajo, O. A., Koval, A., Anandatheerthavarada, H. K., Iqbal, J., Wu, X. Y., Moonga, B. S., Wu, X. B., Biswas, G., Bevis, P. J., Kumegawa, M., Epstein, S., Huang, C. L., Avadhani, N. G., Abe, E., and Zaidi, M. (2002) *FASEB J.* **16**, 302–314
- Uehara, K., Onoue, H., Jeyakumar, L. H., Fleischer, S., and Uehara, A. (2004) *Cell Tissue Res.* **317**, 137–145
- Aon, M. A., Cortassa, S., Wei, A. C., Grunnet, M., and O'Rourke, B. (2010) *Biochim. Biophys. Acta* **1797**, 71–80
- Lin, L., Sharma, V. K., and Sheu, S. S. (2007) *Pflugers Arch.* **454**, 395–402

<sup>3</sup> S. Y. Ryu, G. Beutner, K. W. Kinnally, R. T. Dirksen, and S. S. Sheu, unpublished results.